

# 320-Gb/s Capacity (32 Users $\times$ 10 Gb/s) SPECTS O-CDMA Local Area Network Testbed

V. J. Hernandez, W. Cong, R. P. Scott, C. Yang, N. K. Fontaine, B. H. Kolner, J. P. Heritage, S. J. B. Yoo

*Department of Electrical and Computer Engineering, University of California, Davis, One Shields Ave., Davis, California 95616 USA*

[yoo@ece.ucdavis.edu](mailto:yoo@ece.ucdavis.edu)

**Abstract:** We demonstrate, for the first time, an error-free, 320-Gb/s optical code division multiple access (O-CDMA) network testbed employing the spectral phase encoded time spreading (SPECTS) technique. Results with and without forward error correction (FEC) are presented.

© 2006 Optical Society of America

**OCIS codes:** (060.2330) Fiber optics communications; (999.9999) Optical code division multiple access

## 1. Introduction

Remarkable growth in new high-bandwidth applications such as multimedia entertainment and video conferencing is fueling the need for high-capacity access networking technologies. In particular for flexible bandwidth allocation and simplified network control, optical code division multiple access (O-CDMA) is an attractive technology for use in future high-speed local area networking (LAN) [1]. Several O-CDMA methods have been suggested and demonstrated, but these schemes often require long code lengths (511 chips or greater) to achieve adequate performance [2], are difficult to implement at multi-gigabit rates (by virtue of their time slotting requirements) [3, 4], or are unable to demonstrate high capacity. In this paper, we demonstrate the highest performing O-CDMA testbed to date, supporting 32 users at 10 Gb/s each, for a 320-Gb/s capacity. It employs the spectral phase encoded time spreading (SPECTS) O-CDMA technique [5], whereby phase coding is applied to the spectrum of data-modulated sub-picosecond pulses. Without any forward error correction (FEC), the testbed achieves bit-error-rates (BER) below  $10^{-9}$  for up to 28 users. Utilizing FEC, the testbed can achieve error-free operation (BER  $<10^{-11}$ ) without any apparent noise floor or significant per-user power penalty. These results suggest that an even greater number of users may be supported, and SPECTS O-CDMA can indeed become a viable access technology.

## 2. Testbed Description

In a SPECTS O-CDMA network, each user encodes their broadcast with a unique phase code that is part of an orthogonal (or quasi-orthogonal) set. Encoding causes the pulses to spread in time, and recovery of the pulse (decoding) can only occur if the correct conjugate phase code is applied. The code orthogonality causes all other decoded broadcasts to remain temporally spread as multi-access interference (MAI), and these may be separated from the recovered pulse using optical processing, such as synchronous time gating and/or nonlinear thresholding. Fig. 1 shows the 32-user SPECTS O-CDMA testbed. A mode-locked laser provides a distributed optical carrier for all users, in the form of a 500-fs width pulse train with a 9.95328-GHz repetition rate. A pseudo-random pulse generator (PPG) generates the data used to on-off key (OOK) the optical carrier via a LiNbO<sub>3</sub> Mach-Zehnder modulator. The data may be optionally encoded using an FEC encoder employing a Reed-Solomon code with 6% overhead (RS(255,239)). When FEC is used, the PPG data rate is lowered to 9.250698 Gb/s to maintain a 9.95328-Gb/s rate into the modulator. The modulated optical carrier is distributed to eight SPECTS encoders, which apply 64-chip Hadamard Walsh codes onto the spectrum. The eight encoders nominally provide eight 10-Gb/s users, but time and polarization multiplexing (mux) increases the number of users to thirty-two. The time multiplexer creates two time slots, each 50-ps wide, from the original 100-ps slot. The polarization multiplexer employs a polarization beam combiner (PBC) to create two groups of users, each on an orthogonal polarization. Delays incorporated between the encoder paths and within the multiplexers offset the original data stream by many bit shifts, thereby simulating different data streams from each of the 10-Gb/s users. Signals from all users are combined and sent to a decoder, which selects one of the O-CDMA channels by applying the conjugate phase code. Polarization demultiplexing is performed by the decoder, which contains polarizing elements. Within the O-CDMA receiver module, a nonlinear optical loop mirror (NOLM) time gate and nonlinear thresholder respectively time-demultiplex and suppress MAI.

Coherent interference between the MAI and the correctly decoded pulse can greatly limit the performance of O-CDMA systems, regardless of MAI suppression techniques. In our SPECTS O-CDMA testbed, code selection and synchronous transmission are vital in reducing this interference. The testbed utilizes 64-chip Hadamard Walsh

codes, which ideally yields zero cross-correlation between the MAI and correctly decoded pulse when users transmit synchronously. The MAI is symmetrically displaced away from the decoded pulse, and thus it is desirable to choose codes that yield the maximum displacement. The testbed respectively uses Walsh codes 5, 6, 16, 28, 34, 40, 52, and 54 for Encoders 1 through 8, since these are found to produce the minimum MAI between users [6]. For the measurements below, we use the conjugate of code 5 in the decoder.

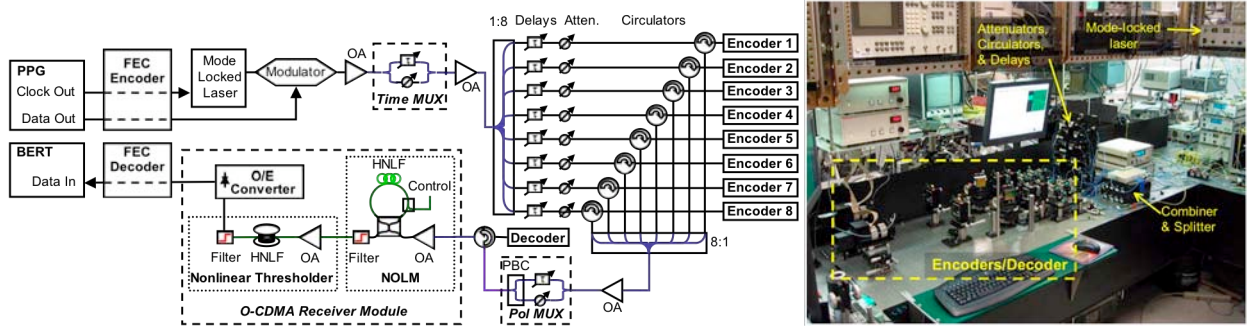


Fig. 1. SPECTS O-CDMA testbed (right) and equivalent block diagram (left). OA: optical amplifier, Atten: attenuators for channel equalization.

### 3. Testbed Performance and Discussion

As stated earlier, optical processing in the testbed requires both time gating and nonlinear thresholding. Fig. 2(a) shows the cross-correlations of the NOLM input and output and it’s effectiveness at rejecting MAI. The gray cross-correlation trace of Fig. 2(a) shows the recovered pulse and MAI produced by the decoder when all thirty-two users transmit. At this point, the received broadcasts have already been polarization demultiplexed, and thus sixteen users remain, divided between two 50-ps time slots. Each time slot clearly shows recovered pulses at  $\pm 25$  ps resulting from correct decoding of code 5 from Encoder 1. As expected from the Walsh codes, the MAI symmetrically surrounds the recovered pulses. The NOLM time demultiplexes the decoder output, successfully selecting the desired time slot, as shown by the black cross-correlation trace of Fig. 2(a). A majority of the MAI within the time slot is likewise suppressed, owing to the NOLM’s narrow gating width of 3 ps. The remaining MAI is reduced using the nonlinear thresholder, whose spectral response is given in Fig. 2(b). The thresholder relies on the high intensity peak power of the recovered pulse to produce self-phase modulation-induced spectral broadening within highly nonlinear fiber (HNLFF). The spectrum of the pulse, centered at 1550 nm, broadens to produce significant spectrum beyond 1560 nm (gray trace). A filter with an edgepass response at 1578 nm (shown as the dashed line) can pass these spectral components through to the optical/electrical (O/E) converter for final detection. Suppression of MAI by the thresholder is demonstrated by removing Encoder 1 (code 5) from the system, such that only MAI from the remaining 28 users is present. Under this condition, the MAI out of the NOLM will not be able to generate high peak powers, and no spectral broadening occurs (black trace). As a result, very little MAI spectrum passes through the filter, and the O/E converter detects negligible MAI power.

The BER performance of the testbed (using PRBS length  $2^{31}-1$ ), with and without FEC, is shown in Fig. 3. The data are presented versus power per user as measured at the input of the O-CDMA Receiver Module. The back-to-back case represents the system performance from the modulator directly to the O-CDMA receiver module, bypassing all multiplexers, encoders, and the decoder. The remainder of the measurements successively adds encoders to the system with the multiplexers in place, such that each added encoder represents four additional users (1 O-CDMA code  $\times$  2 time slots  $\times$  2 polarizations). When FEC is not used (FEC encoder and decoder are removed from the system), the results are as shown in Fig. 3(a). For up to 28 users, the system is able to perform with BER  $< 10^{-9}$  with an increasing noise floor. As stated above, this noise floor results from coherent interference between the signal and MAI. Considerably worse performance would be expected if the thresholder were not used. The noise floor ultimately yields BER  $< 10^{-8}$  for the 32-user case and a per user penalty of 13 dB (BER =  $10^{-9}$ ) between the 4- and 28- user cases. Dramatic improvement is achieved when FEC is incorporated, as shown in Fig. 3(b). In this case, the BER floor is eliminated such that the testbed can remain error free for a period of 240 billion bits (BER  $< 10^{-11}$ ) with up to 32 users. The arrows at the end of each BER curve indicate the minimum power required to achieve error-free operation for a given number of users. The per-user power penalties are likewise reduced when using FEC, such that the total penalty between four and thirty-two users is only 4.5 dB at BER =  $10^{-9}$  (0.16 dB penalty per user). Fig. 4 also shows the eye diagram for various users, measured at the final data point (or error-free point) of the BER curves. Without FEC, a 15 GHz-bandwidth O/E converter is used in the testbed, yielding the return-to-zero (RZ) eye diagrams of Fig. 3(a). When FEC is added, the system uses a separate O/E converter,

capable of converting the received RZ data into the non-return-to-zero (NRZ) format required by the FEC circuitry. The eye diagrams of Fig. 3(b) show the output of the O/E converter, and these show considerably more noise since they are measured at lower input signal powers. The effectiveness of the FEC is demonstrated since such eye diagrams can yield error-free performance, despite the added noise. The improvements illustrated in the BER and eye diagram measurements are promising as it indicates that many more users may be accommodated by the testbed with minimal performance degradation.

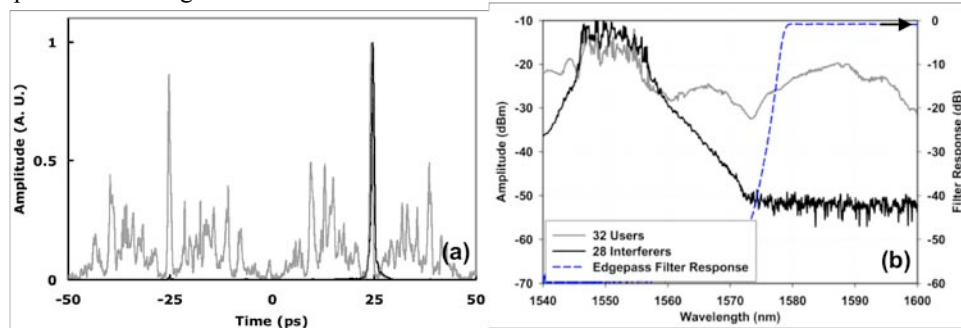


Fig. 2. (a) Cross-correlation of correctly decoded pulse and MAI before (gray trace) and after the NOLM time gate (black trace). (b) Spectral response of nonlinear thresholder.

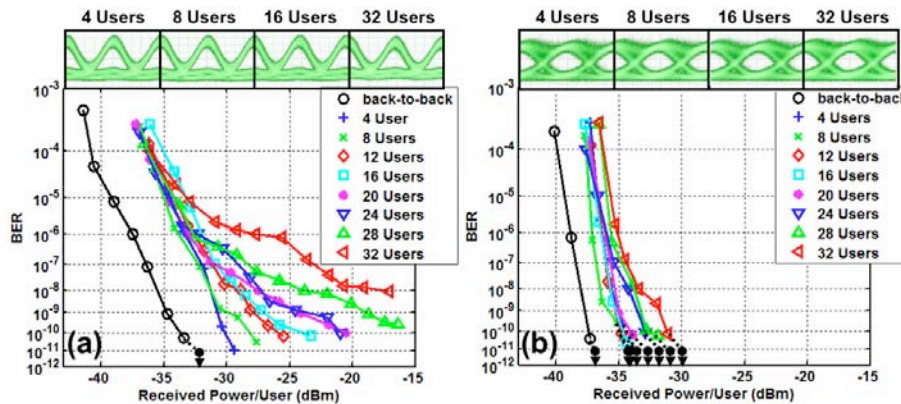


Fig. 3. Bit-error-rate measurements and eye diagrams of the 10-Gb/s/user testbed (a) with FEC and (b) without FEC.

#### 4. Conclusion

We have demonstrated the first error-free SPECTS O-CDMA network testbed with 32 simultaneous users, each operating at 10 Gb/s. Successful employment of time and polarization multiplexing increase the total demonstrated throughput to 320 Gb/s while utilizing just eight encoders. FEC enables error-free operation of the testbed with a minimal per-user power penalty and no apparent noise floor in the BER performance. Without FEC, the testbed is still able to achieve  $\text{BER} < 10^{-9}$  for 28 users and  $\text{BER} < 10^{-8}$  for 32 users. The excellent BER performance of the testbed results from outstanding suppression of MAI for an increasing number of simultaneous users.

#### References

1. A. Stok and E. H. Sargent, "The role of optical CDMA in access networks," *IEEE Commun. Mag.* **40**, 83-87 (2002).
2. X. Wang, *et al.*, "Demonstration of 12-user, 10.71 Gbps truly asynchronous OCDMA using FEC and a pair of multi-port optical-encoder/decoders," presented at the European Conference and Exhibition on Optical Communication, Glasgow, UK, Sept. 25-29, 2005.
3. J. Faucher, *et al.*, "Multiuser OCDMA system demonstrator with full CDR using a novel OCDMA receiver," *IEEE Photon. Technol. Lett.* **17**, 1115-1117 (2005).
4. V. Baby, *et al.*, "Experimental demonstration and scalability analysis of a four-node 102-Gchip/s fast frequency-hopping time-spreading optical CDMA network," *IEEE Photon. Technol. Lett.* **17**, 253-255 (2005).
5. A. M. Weiner, *et al.*, "Encoding and decoding of femtosecond pulses," *Opt. Lett.* **13**, 300-302 (1988).
6. R. P. Scott, *et al.*, "An eight-user time-slotted SPECTS O-CDMA testbed: demonstration and simulations," *J. Lightwave Technol.* **23**, 3232-3240 (2005).

This work was supported in part by DARPA and SPAWAR under agreement number N66001-02-1-8937 and by the AFOSR through the UC Davis Center for Digital Security.